EARTH SURFACE PROCESSES AND LANDFORMS
Earth Surf. Process. Landforms (2020)

Published online in Wiley Online Library
(wileyonlinelibrary.com) DOI: 10.1002/esp.5002

Relative quantification of wind erosion in argan woodlands in the Souss Basin, Morocco

Miriam Marzen,[1]* Mario Kirchhoff,[1] Irene Marzolff,[2] Ali Aït Hssaine[3] and Johannes B. Ries[1]
[1] Department of Physical Geography, Trier University, Trier DE-54286, Germany
[2] Department of Physical Geography, Goethe University Frankfurt am Main, Frankfurt am Main DE-60438, Germany
[3] Department of Geography, Université Ibn Zohr, Agadir MA-80060, Morocco

Received 6 April 2020; Revised 1 September 2020; Accepted 2 September 2020

*Correspondence to: Marzen Miriam, Department of Physical Geography, Trier University, DE-54286 Trier, Germany. E-mail: mmarzen@uni-trier.de

ESPL
Earth Surface Processes and Landforms

ABSTRACT: The endemic argan woodlands cover large parts of South Morocco and create a characteristic landscape with areas of sparsely vegetated and bare soil surfaces between single trees. This unique ecosystem has been under extensive agrosilvopastoral management for centuries and is now at risk of degradation caused by overgrazing and increasing scarcity and variability of rainfall.

To investigate susceptibility to wind erosion, we conducted an experimental–empirical study including wind tunnel tests and a drone-generated digital elevation model and quantified wind-erodible material on five different associated surface types by means of sediment catchers. The highest emission flux was measured on freshly ploughed surfaces (1875 g m^{-2} h^{-1}), while older ploughed areas with a re-established crust produced a much lower emission flux (795 g m^{-2} h^{-1}). Extensive tillage may have been a sustainable practice for generations, but increasing drought and uncertainty of rainfall now lead to an acute risk of severe soil erosion and dust production. The typical crusted surfaces characterized by residual rock fragment accumulation and wash processes produced the second highest emission flux (1,354 g m^{-2} h^{-1}). Material collected from tree-shaded areas (933 g m^{-2} h^{-1}) was revealed to be a considerable source of organic material, possibly affecting substrate conditions positively on a larger regional scale. The lowest flux was measured on rock fragment-covered surfaces (301 g m^{-2} h^{-1}).

The data show that open argan woodland may be a considerable source for wind erosion and dust production, depending on surface characteristics strongly related to management. An adapted management must include the conservation of argan trees to offer a promising approach to prevent severe wind erosion and dust production and mitigate possible impacts of land-use change and climate change related shifts in wind and rainfall patterns. © 2020 The Authors. Earth Surface Processes and Landforms published by John Wiley & Sons Ltd

KEYWORDS: Wind erosion; experimental geomorphology; argan trees; dryland environments; soil degradation

Introduction

The Souss-Massa Region is the remaining natural habitat of the endemic argan tree (*Argania spinosa* (L.) Skeels). The argan tree is one of the very few woody species adapted to survive in the extreme conditions of semi-arid to arid environments, creating a characteristic open woodland over an area of about 950,000 ha (Le Polain de Waroux and Lambin, 2012; Lefhaili, 2015). It is the keystone species for the regional ecosystem as well as the basis for production of argan oil, which is sold worldwide with growing demand. Because of their spatial distribution along the peripheries of the Sahara, argan woodlands are assumed to act as a buffer against desertification (UNESCO, 2015), thus protecting the fertile and productive agricultural regions located in the Souss-Massa Region. UNESCO designated a biosphere reserve of 2,568,780 ha with the core area in the Souss-Massa National Park under the Man and the Biosphere (MAB) program in 1998 (UNESCO, 2002) and added its traditional management to the Intangible Cultural Heritage (ICH) program in 2014. Despite these acknowledgements of the ecological and socio-economic implications and the high level of societal interest and regional and national actions, argan woodlands are severely threatened by degradation processes. The main causes are an extremely diminished rejuvenation of argan populations and overexploitation of adult trees by overgrazing (Lybbert *et al.*, 2010; Le Polain de Waroux and Lambin, 2012; Kirchhoff *et al.*, 2019a). In this vulnerable environment, wind erosion and dust emission are potentially major degradation processes that remain largely unassessed. On-site and off-site effects of wind erosion and dust emission are great challenges to scientists, politicians and food producers alike and among the most urgent ecological and economic issues in the early twenty-first century (e.g. Montanarella *et al.*, 2016; Middleton, 2017). In 1996, the United Nations launched the Convention to Combat Desertification (UNCCD) and have since spent over $130 million on programs for sustainable land management. The semi-arid

[Correction added on 09 November 2020 after first online publication: The article title has been updated in this version.]

and arid regions of North Africa are considered main dust sources on a global scale (Bullard and Baddock, 2019), and desertification as defined by the UNCCD threatens the greatest part of Morocco (Bouabid *et al.*, 2010). One part of the convention is the National Action Plan (AGR/DAF Report, 2002). It identifies the southeast, southwest and oriental regions as the most threatened by wind erosion, with the southerly Chergui and Sirocco winds strongly impacting the lower Valley of Drâa, Tafilalet and the irrigated plains of Souss-Massa, where our study site is located. The effects of wind erosion and dust emission include severe ecological and socio-economic consequences. Among them are reduced soil fertility by deflation of soil particles, corrasion damage to young plants and infrastructure, contamination of drinking water and direct health risks associated with dust emission (e.g. Goudie, 2014; Duniway *et al.*, 2019). While extreme wind events are recognized as severe natural hazards (e.g. Hoffmann *et al.*, 2011), wind erosion events caused by comparably low wind velocities may happen on a large scale but remain mostly unnoticed (Chepil, 1960; Chepil and Woodruff, 1963; Funk, 2016). The recent IPCC Special Report (IPCC, 2019) defines land use and land-use change as major triggers of global soil erosion and land degradation and points out the crucial role of appropriate land management to mitigate climate change effects. The Souss Basin is a region where the natural habitat and traditional land management have been closely intertwined for millennia, with evidence that geomorphological activity increased with increasing human impact in the course of population growth around 700AD (McGregor *et al.*, 2009). It exhibits several factors that can trigger aeolian transport, such as aridity, loamy soils and substrates, sufficient wind energy and unobstructed areas that increase the air stream's erosive energy.

In this vulnerable environment, soil erosion is a potential cause as well as consequence of degradation and desertification, but measurements to quantify recent rates are rare and none focus on wind erosion.

Our research question and research hypotheses RH1–3 are based on the mentioned research gaps concerning the lack of data on the wind erosion potential in this specific dryland environment at the fringes of the Sahara Desert.

The research question of this study is: How do specific surface characteristics related to the environment influence the susceptibility of open argan woodlands to wind erosion and dust emission?

RH1: The argan woodland environment comprises different surface types with corresponding specific surface characteristics.

We identify, describe and map the different surface types that are typical for the regional argan woodland environment and subsequently determine their erodibility by wind.

RH2: The potential wind erosion of and dust emission from the argan woodland environment are not uniform across the entire area but differ according to surface type.

By comparing emission values, we relatively quantify the potential wind erosion associated with each surface type.

RH3: Material collected from wind erosion tests is significantly related to substrate and surface characteristics.

Erodible material collected from all surface types is tested for potential relations with quantified plot-specific substrate and surface parameters.

Materials and Methods

Location and test site

The study area is located to the north of Taroudannt in the Souss-Massa Region in south Morocco (Figure 1). The Souss Basin (30–31°N and 7–9°W) is traversed by the river Oued Souss and framed by the High Atlas to the north with Palaeozoic, Mesozoic and Cenozoic rocks and the Anti-Atlas to the south with Precambrian and Palaeozoic rocks (Hssaisoune *et al.*, 2016).

The Souss Basin has been shaped by many alluvial and coalescing fans with Pliocene–Quaternary fluvial, fluvio-lacustrine and aeolian sediments (Aït Hssaine and Bridgland, 2009; Chakir *et al.*, 2014) on which mostly raw regosols, fluvisols and calcaric fluvisols (Jones *et al.*, 2013) have developed. The geomorphological evolution of the Piedmont in the Taroudannt region is described by Aït Hssaine (2000). The climate is arid with 20°C mean annual temperature with a significantly increasing trend, and a constantly negative water balance (FAO AQUASTAT, 2015). Annual precipitation is 200mm with very high variability and shows a severe downward trend (–3% to –30% over the period 1976–2006) with an increase in the maximum duration of dry periods (+15days) since the 1960s (National Meteorology Directorate Morocco, 2007 in Houzir *et al.*, 2016).

The Souss Plain is one of the most productive agricultural regions of Morocco. The change in cultivation to fruit-tree plantations and irrigated greenhouses as well as uncontrolled livestock grazing has resulted in high land-use pressure and dynamics. The geomorphological consequences of intense agricultural pressure combined with increasing water scarcity range from intensified gully and badland development to a sinking groundwater table, severely affecting this vulnerable environment (Kuhn *et al.*, 2010; Peter *et al.*, 2014; Ait Kadi and Ziyad, 2018; Hssaisoune *et al.*, 2020).

The 100m × 100m test site IRG1c is part of a larger research area situated on an alluvial fan, formed by Wadi Irguitène originating from the High Atlas in the north (Kirchhoff *et al.*, 2019a; Kirchhoff *et al.*, 2019b). It belongs to the remaining natural habitat of the argan tree *Argania spinosa*, which can be assumed to be a paramount keystone species in this environment. Besides the trees, little other vegetation remains due to scarce rain and temporarily intense browsing pressure. The traditional agrosilvopastoral land use includes harvesting of argan fruit, pasture for browsing animal herds and traditional speculative rainfed agriculture between the single trees. The two main wind directions measured at Taroudant airport are south-southwest and east-northeast (Figure 2). Mean wind velocities suggest the potential for wind erosion throughout the whole year, which was also evident during the fieldwork on-site.

Surface types and test plots

We defined five different surface types associated with open argan woodlands at the test site. The criteria used to define the surface types were geomorphological features concerning surface characteristics that affect erodibility by wind, such as roughness and vegetation/rock fragment cover. Surface roughness often corresponds to key geomorphological factors such as surface crust, rock fragment cover, vegetation and flow path development and is of particular importance for experimental studies on a small scale (Darboux *et al.*, 2002). The surface

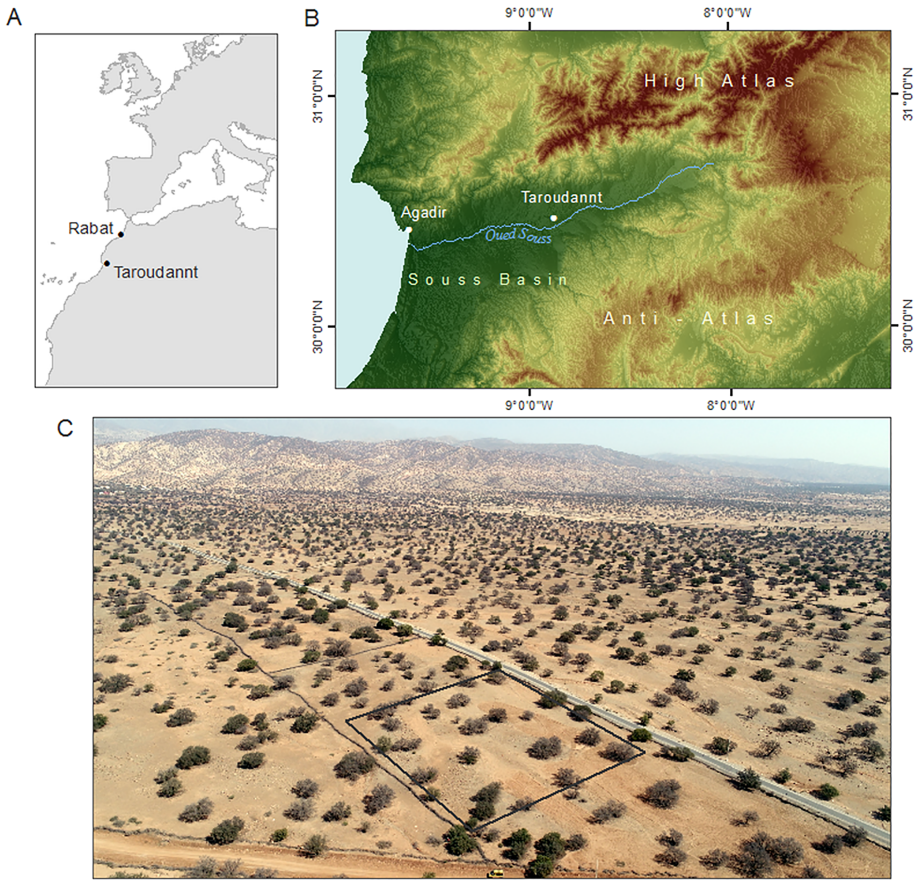

Figure 1. (A, B) Location of the study area near Taroudannt, South Morocco. (C) Argan woodland environment with test site (1 ha) outlined in black frame, view towards north-east [Colour figure can be viewed at wileyonlinelibrary.com]

types can be considered representative of argan woodland areas of south Morocco, particularly on alluvial fans in the Souss Basin. For each of the five surface types, three representative test plots oriented along the main wind directions were chosen for the experimental procedure. For digital mapping of the 1 ha test site, vertical and oblique imagery taken with a quadcopter UAV (DJI Phantom 4) were used to generate 3 cm-resolution digital surface and terrain models (DSMs/DTMs) and a 1.5 cm-resolution orthophoto mosaic by means of structure-from-motion (SfM) photogrammetry using Agisoft Metashape 1.5 (Stephan *et al.*, 2019). The 'tree area' class, corresponding to the surface area covered by the tree crown, was mapped automatically from a crown height model (computed as DSM minus DTM) using ESRI ArcGIS 10.7. All other classes were mapped manually based on visual interpretation of the orthophoto and DTM-derived hill-shade map.

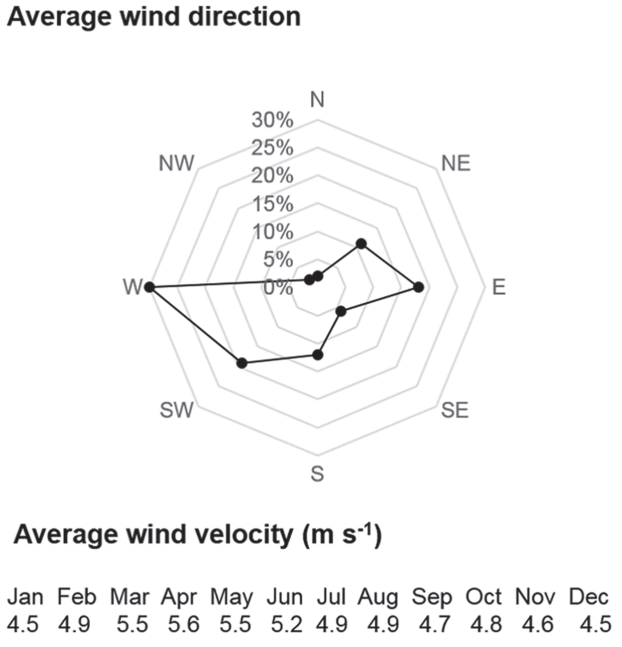

Figure 2. Wind data from Taroudannt Airport weather station, 2009–2019 (source: weatheronline.co.uk)

Experimental device and procedure

Tests were conducted using the Trier Portable Wind and Rainfall Simulator without the rainfall equipment (Figure 3A). This device is suitable for studying the effects of a steady-velocity wind stream on autochthonous surfaces. The wind tunnel's test section measures 4 m × 0.7 m and contains an open floor area of 2.2 m^2 in order to test the largely undisturbed soil surface on-site. The air stream is generated by a rotor-type fan, led through a 4 m-long transition section and a honeycomb in order to generate a quasi-laminar air flow. The resulting air stream proved reliably stable in terms of the temporal and spatial variability of wind velocities and shows a logarithmic wind velocity profile up to 0.15 cm height. The average wind velocity was 7.5 $m s^{-1}$ at 0.3 m height, controlled by means of an anemometer. Compared with natural conditions, the produced wind ranges at a comparably low intensity of 5 on the Beaufort scale ('fresh breeze'), which is adequate for wind erosion processes to be initiated (e.g. Bagnold, 1941; Kok *et al.*, 2012), and is steady, whereas natural wind is characterized by gusts. The physical limitations of the device concerning its temporal and spatial scale lead to great differences from natural conditions

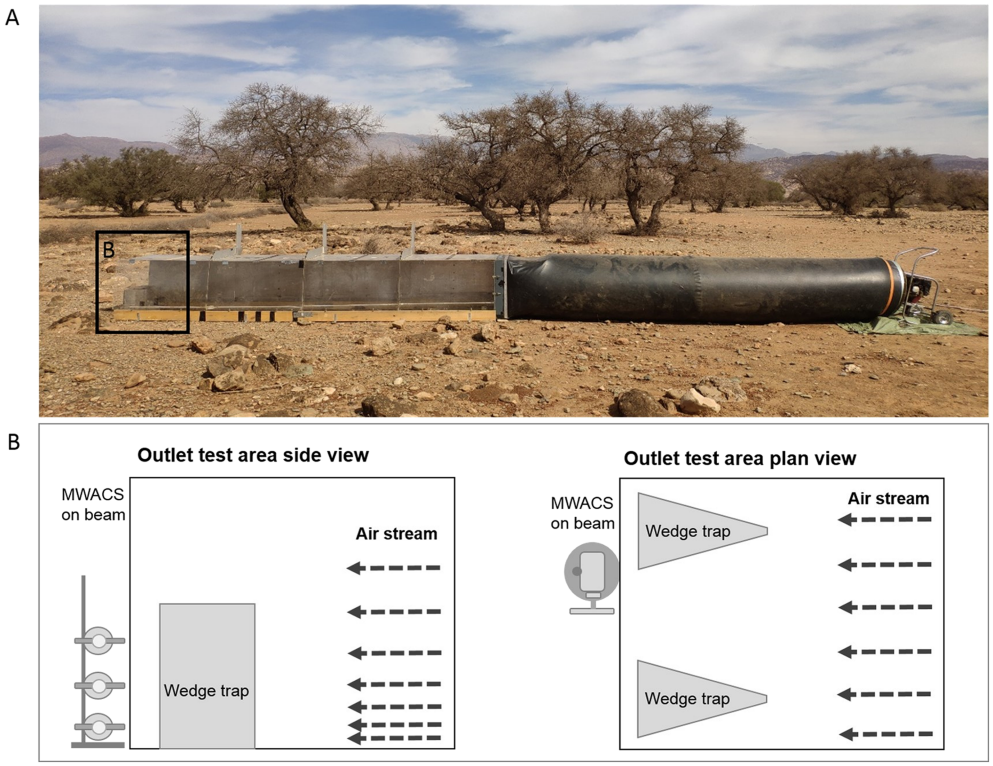

Figure 3. (A) The Trier portable wind simulator on site; (B) outlet area with collectors. [Colour figure can be viewed at wileyonlinelibrary.com]

concerning the extent of the processes involved, subsequently leading to differences in measured material. The erosivity of the resulting air stream and the subsequently transported material may be considered to be located at the lower end due to these physical limitations. The main value of this experimental device relates to the opportunity to study soil and substrate surfaces on-site, which includes an undisturbed and intact surface structure. This is particularly important for wind erosion studies, where even small errors in the experimental setup (caused by e.g. slight destruction of the surface structure during transport for laboratory studies) can lead to substantial errors in the results due to generally small measurement values. The data derived from the wind tunnel tests described herein are therefore a valuable compromise, particularly for regions where continuous monitoring has not been possible or where reliable data are generally scarce. Further details about the experimental setup concerning the spatial distribution of the velocity of the wind field may be found in Fister *et al.* (2012) and Wirtz *et al.* (2020). The experimental setup's physical limitations concerning reliability, validity and upscaling as well as adequate application of experimentally derived results are addressed in Iserloh *et al.* (2013) and Marzen *et al.* (2017).

The measurement procedure described here allows for a relative comparison between plots and sites, since the velocity of the air stream is a fixed parameter and reliably reproducible.

For each surface type, three different plots were chosen to collect data reflecting the natural variability of test plots and allow for simple statistical investigations. The test duration was 10 min per run. Material detached from the test area was collected by means of modified Wilson and Cook (MWAC, Wilson and Cooke, 1980) samplers at three different heights and two wedge traps (WTs, Fister *et al.*, 2012) (Figure 3B). To keep the disturbance of the air stream as low as possible, the traps were positioned offset with respect to each other (Figure 3B). We applied two different types of collector, where one mainly collects finer airborne material and the other coarser material. MWACs were mounted with openings at 4.0 m in the flow direction (the end of the tunnel and test section) at heights of 0.02, 0.10 and 0.20 m on a beam to collect material airborne by saltation, modified saltation and short-term suspension. Trap efficiency was found to be very good for sand and fine sand size classes (Goossens *et al.*, 2000; Goossens *et al.*, 2018) but poorer for finer classes and particulate matter (Mendez *et al.*, 2016). The two WTs were positioned with the opening attached to the ground at 3.7 m distance in the flow direction from the start of the test section to collect material transported by processes of reptation/surface creep, saltation, modified saltation and short-term suspension.

Collected material was weighed by means of precision scales. The total transported material (g) was calculated by subtracting the weight of the collector before from the weight after the experiment. The horizontal emission flux q ($g m^{-2} h^{-1}$) was calculated by dividing the mass values (g) by the collector opening and the duration of the experiment. The collector openings were 0.000028 m^2 for the MWACs and 0.006 m^2 for the WTs.

To estimate the temporal development during a potential wind erosion event and the potentially available material, a second run was carried out on each plot in a sequence (run 1 and run 2) and with mounted wedge traps. Experiments were performed on all surface types but not spread over the total area in order to keep destruction and disturbance to a minimal level (Figure 4).

The results obtained using both types of trap are presented and interpreted together, and also related to each collector type due to the different erosion processes involved. MWACs have highest efficiency for fine grain sizes, and the results can be considered to represent dust emission including very small particles affecting human health. Wedge traps collect larger grain sizes that are not airborne but move via reptation, and the results tend to strongly underestimate fine size classes due to the collection procedure, which involves the opening and

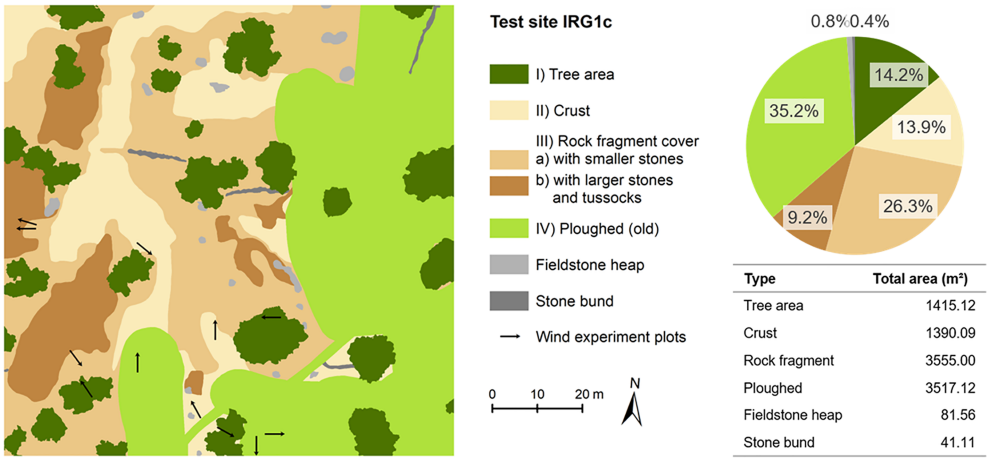

Type	Total area (m²)
Tree area	1415.12
Crust	1390.09
Rock fragment	3555.00
Ploughed	3517.12
Fieldstone heap	81.56
Stone bund	41.11

Figure 4. Map of surface types on test site, based on orthophoto mosaic and digital terrain model derived from UAV-based aerial photography (November 2019). Surface type V (freshly ploughed) was not originally present in the field but was simulated on the wind experiment plots located in ploughed (old) type. [Colour figure can be viewed at wileyonlinelibrary.com]

cleaning of traps. Since the highest proportion of wind-eroded material is transported via surface creep, and a total of 60% in the first 0.06 m (Chepil, 1945), these relations might differ, and it can be expected that differences will increase with higher surface roughness. We therefore interpret the results accordingly to provide a realistic approximation of the total potential on-site emission flux.

Soil and surface parameters

We estimated the percentage cover of litter, rock fragments, crust and vegetation on the plot by visual observation. Inclination and orientation were measured using an inclinometer and compass. The surface roughness of the test plots was measured with a roller chain on-site after Saleh (1993) as $C_r = (1 - L_2/L_1) \times 100$, where L_1 is the chain length and L_2 is the plot length. The surface roughness was also computed for all surface types from the DTM as the ratio of true surface area to planimetric area (Jenness, 2013), which was chosen because it corresponds to the C_r coefficient (Saleh, 1993) applied on-site. The surface area ratio computed for a test site can be expected to be slightly biased towards rougher surfaces, as the 3 cm resolution of the DTM smoothens out some of the finer-scaled structures. Shear strength was measured using a pocket vane test device (Eijkelkamp, product code 14.10) and is given as the mean of ten tests per surface type. Samples for soil analysis were collected at depth of 0–0.05 m, air dried and sieved for fine fraction (< 2 mm). We measured gravimetric soil water content (%), particle size distribution after Köhn (1929) and percolation stability by means of a Mariotte bottle and corrected for total sand (Auerswald, 1995; Mbagwu and Auerswald, 1999). SOC was derived by means of a Euro CHNS 3000 elemental analyser by HEKAtech. Other parameters that have been found to be crucial for wind erosion such as substrate water content (e.g. De Oro *et al.*, 2019) and air humidity (e.g. Ravi *et al.*, 2004) were both constant during the field tests.

Statistical analysis

A Shapiro–Wilk (SW) test was performed to test the data per dataset and per surface type for normal distribution, and Spearman rank coefficient analyses were performed per collector type (both/total; MWACs; wedge traps) to test for relationships between the collected material and the soil and surface parameters. The SW test, Spearman's rho and boxplots were derived using SPSS 25 (IBM Corp., 2017).

Results

Characteristic surface types within the argan woodland environment

To investigate RH1, we identified, described and mapped the different surface types that are typical for the regional argan woodland environment and quantified their substrate and surface characteristics.

Four different surface types were distinguished on-site and digitally mapped: (I) tree area, (II) crust, (III) rock fragment cover with (a) smaller rock sizes and (b) larger rock sizes and tussocks, and (IV) ploughed (old) (Figure 4).

Of the total area (1 ha), the surface types with rock fragments and ploughed (old) accounted for the greatest fractions, with 35.5% and 35.2% overall, respectively. Tree area (14.2%) and crust (13.9%) together made up one-third of the total area. A minor percentage was covered by fieldstone heaps and stone bunds that were patchily distributed over the non-ploughed area but were not tested for wind erodibility.

Photographs of the respective test surfaces are shown in Figure 5. Soil and surface characteristics estimated and measured on-site are presented in Table I.

I Crust

The specific consideration of tree areas follows Kirchhoff *et al.* (2019a), who found tree cover to be a general feature establishing chemical and physical soil surface traits in argan woodlands. We defined this surface type as the area directly underneath the crown and mapped them automatically from a crown-height model. The tree area made up 1,415 m^2 of the total area. The most notable characteristic of this area's surface at the time of our experiments in early October 2019 was a very high percentage of litter that was shed in summer. This litter cover consisted of small lanceolate leaves that form quite hard pins when dried. The area was also covered with a relatively high percentage of cohesionless substrate. The surface showed relatively high roughness values caused by large rock fragments that accumulate due to goat kicks and as the shepherds throw them to knock down argan nuts.

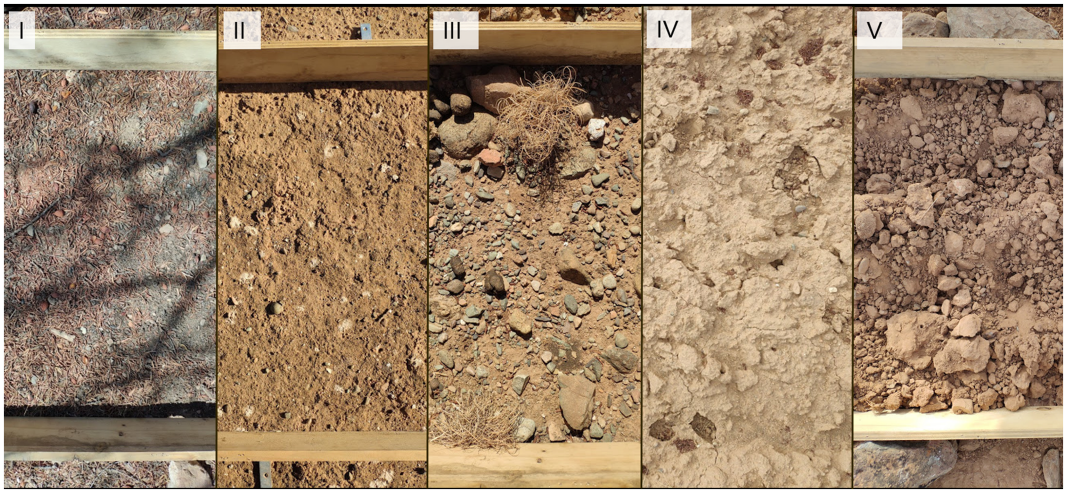

Figure 5. Test plots representing the five tested surface types: (I) tree area, (II) crust, (III) rock fragment cover, (IV) ploughed (old) and (V) freshly ploughed [Colour figure can be viewed at wileyonlinelibrary.com]

II Crust

The crusted surface (1,390 m^2) was covered with a 0.01–0.02 m strong crust with only small, mostly embedded rock fragments that originate from residual accumulation. The top layer of the crusts was mainly biological, with a smaller proportion of physical crust and a shear resistance much higher than that of the underlying substrate. This surface type seemed to be strongly influenced by wash processes during medium to heavy rain events. The crust area covered 13.9% of the total area and displayed the lowest and least variable roughness due to its comparative lack of large rock fragments.

III Rock fragment cover

The rock fragment cover areas had a high percentage of smaller and larger rock fragments with a notable high portion of fine and medium gravel including very coarse pebbles (type IIIa) as well as coarse gravel including cobbles and single boulders (type IIIb). Type IIIa in particular appeared as a typical desert pavement. Along with the distinct fieldstone heaps and stone bunds, the rock fragment cover probably developed during selective tilling and casual land-clearing activities by stone dumping. This is a common practice on agriculturally managed land and may here be associated with the cultivation of wheat. Once these areas were covered with rock fragments, it was less likely that the farmer would lead the plough over the area, and disturbance was strongly reduced. Pebbles and cobbles embedded at various depths in the fine material suggest that these places have been used in this manner for a long time. (Grazed) tussock grass and entrances to animals' tunnels were also found particularly on type IIIb, indicating a general low level of disturbance except by animal herds. The presence of small to large rock fragments and tussock tufts scattered over the otherwise rather flat crust area resulted in the highest roughness variability in this class, which covered a great share of the total test site (3,555 m^2).

IV Ploughed (old)

A great part of the area of the test site was found ploughed. Satellite imagery (PlanetScope) allows to date the last ploughing to November 2018, one year previously. The simultaneous use of areas covered by argan trees for speculative cultivation of grains is a traditional practice in south Morocco. In the prospect of imminent autumn rains, the area is ploughed. The seeds sown germinate with comparably small amounts of precipitation, which also generates a fresh sealing and crusting of the broken substrate. After ploughing and subsequent sowing in autumn 2018, however, the lack of sufficient rainfall in the summer and autumn of 2019 resulted in a suspension of the cultivation cycle. One year later, the ridge–furrow pattern appeared untreated but settled, and a 0.5–1 cm thick, rather loose physical crust with a high content of voids had developed during the past year due to raindrop impact. The ploughed area covered the second largest share of the test site with 3,517 m^2.

V Freshly ploughed

The area of type IV, ploughed (old), has potentially been ploughed annually for a long time in the past and will probably be reactivated at some point. Since there was no ploughing in 2019, we simulated the ploughing procedure to measure the erodible material available on freshly ploughed surfaces. After the experiments on surface type IV, ploughed (old), we used a shovel to break the physical surface crust, destroying larger aggregates and forming the typical ridge–furrow pattern on the same plot as tested on surface IV. The crusted substrate tended to break into large aggregates that led to a high surface roughness besides the generation of cohesionless fine substrate.

Soil and surface parameters

The mean soil and surface parameters are presented according to each surface type in Table I. The results for the soil parameters for ploughed (old) and freshly ploughed areas are the same due to the test procedure. The soil type for the entire test area was a weakly developed Regosol with loamy texture and 48% sand, 35% silt and 17% clay (mean values). The mean surface characteristics showed that the tree area was the only site with a high percentage of litter cover (52%) and a comparably high percentage of loose fine material (11%), while the rock fragment type consisted mainly of embedded and loose rock fragments (80%) and crusted surface (10%). The crust surface type mainly consisted of crust and rocks (78% and 20%, respectively), resembling the ploughed (old) surface (65% and 25%, respectively) but with differences in crust thickness and shear strength, with 2.5 $kg\,cm^{-2}$ for crust and 1.2 $kg\,cm^{-2}$ for ploughed (old). The freshly ploughed surface had the highest percentage of loose sediment (63%), also showing a high fraction of rock fragments (32%). The highest shear strength values were measured for rock fragments (>2.7 $kg\,cm^{-2}$) and

Table I. Plot surface and substrate characteristics for the five surface types

		Surface parameters (mean)							Substrate parameters (mean)					
							Roughness							
Surface/Unit	Exp.	Litter (%)	Veg. (%)	Crust (%)	Grain <2mm (%)	Rock fragments (%)	(C_r index)	(surface/area ratio)	Shear strength (kg cm^{-2})	fine soil (<2mm) (%)	coarse soil (>2mm) (%)	Soil moisture (%)	Percolation stability (ml/10min)	SOC (%)
Tree area	S-W	52	0	15	11	23	4.3	1.0161	1.1	92.37	7.63	1.23	63.30	3.60
Crust	N-NE	0	0	78	2	20	5.5	1.0059	2.5	88.76	11.24	1.29	5.29	0.49
Rock fragments	NW-N	5	5	10	0	80	7.8	1.0123	>2.7	68.69	31.31	1.13	23.31	0.78
Ploughed	N-S-E	5	0	65	5	25	14.7	1.0127	1.2					
Freshly ploughed	N-S-E	2	0	3	63	32	21.1	NA	0.1	92.83	7.17	1.21	5.42	0.53

crust (2.5 kg cm^{-2}). The lowest shear strength (0.5 kg cm^{-2}) was measured on the freshly ploughed surface type.

The surface types mapped on the test site (Figure 4) are clearly differentiated by their different surface roughness (Figure 6). Among the tested surfaces, the highest roughness values were found for rock fragments with larger rocks and tussocks, type IIIb (μ = 1.022, σ = 0.048). Tree area also showed a high roughness index (μ = 1.016) due to the presence of large rocks, while the lowest and least variable roughness values (μ = 1.006, σ = 0.010) were found for the crust type.

Soil substrates showed pronounced differences in several parameters despite their high spatial proximity. Coarse soil (>2 mm) was found to be high on the rock fragment type (31.31%), while the other surface types showed percentages below 12%. Low percolation stability was measured for the ploughed (old)/freshly ploughed (5.29 ml/10 min) and crust surface types (5.42 ml/10 min) and was highest for tree area (63.30 ml/10 min). The second highest stability was measured for rock fragment cover (23.31 ml/10 min). Soil organic carbon (SOC) was found to be very low on all test plots except tree area (3.60%), which coincides with the high percolation stability and medium shear strength (1.1 kg cm^{-2}). On all other types, SOC values were very low (0.49–0.78%).

Susceptibility to wind erosion and dust emission across surface types

To investigate RH2, we performed 30 wind erosion tests at the argan woodland test site. Three tests were performed on each of the five surface types with MWACs and WT applied (run 1), and a second run for each test with only WT (run 2). On all tested surfaces, material available for wind erosion was collected. The values are displayed based on a combined calculation for both trap systems (Figure 7A) as well as separately per collector system for MWACs (Figure 7B, 8 and 9) and WT (Figure 10).

Results from both collector systems added and compared

To calculate the mean values from both collector systems, MWACs and WT data from run 1 were analysed together (Figure 7A) and are displayed for comparison in Figure 7B. Exact values are presented in Table II.

The mean horizontal emission fluxes derived by adding the substrate yield from both collector systems showed clear differences between the surface types. Freshly ploughed sites produced the highest mean fluxes (1,872.48 g m^{-2} h^{-1}), followed by crust (1,353.78 g m^{-2} h^{-1}), tree area (932.93 g m^{-2} h^{-1}), ploughed (old) (794.75 g m^{-2} h^{-1}) and rock fragments (301.12 g m^{-2} h^{-1}). Results from wedge traps and MWACs showed similar trends in their general relative distribution but differed in some cases (Table II).

The differences in collector efficiency were most notable for freshly ploughed surfaces, caused by the relative lack of creeping particles due to the high roughness, while airborne material was efficiently collected by MWACs. The high values for tree areas measured using WT were caused by a high percentage of organic material, i.e. dry argan leaves and argan fruit fragments not collected by MWACs. Generally, the MWACs displayed greater differences between the surface types.

MWAC sampler-collected material

Figure 8A shows the differences in mean emission between all the surface types. The highest emission fluxes were measured for the freshly ploughed and crust surface types with 1,840.63 and 1,325.88 g m^{-2} h^{-1}, respectively. The rock fragment cover produced the lowest flux (296.37 g m^{-2} h^{-1}). Tree area (779.93 g m^{-2} h^{-1}) and ploughed (old) (764.33 g m^{-2} h^{-1}) produced similar rates but with differences in the vertical distribution pattern (Figure 9).

The range of values per height was quite small for most surfaces, except for freshly ploughed (Figure 8B, Tables II and III). In particular, the ploughed (old) surfaces showed remarkably little variance with height but also produced much smaller values. All measurements showed a vertical transport pattern with reduced values at increasing height (Figure 9), which is in line with findings from other studies carried out with vertically mounted catcher systems (e.g. Dong *et al.*, 2003; Leys and McTainsh, 1996). For tree area, rock fragments and crust, a strong decrease with height was found.

The mean vertical transport was best explained by an exponential function for tree area (R^2 = 0.99) and a linear function for crust (R^2 = 0.97). Rock fragments (R^2 = 0.98) and both tilled surface types, i.e. ploughed (old) and freshly ploughed, were best fit by power functions (both R^2 = 0.98). Due to the small number of measurement points (three per test), the proposed functions and coefficients of determination are only given as a general trend.

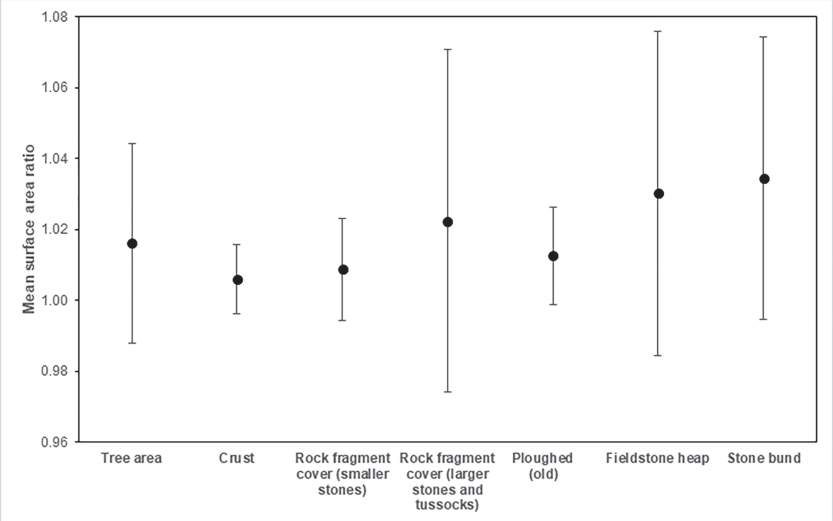

Figure 6. Mean (dots) and standard deviation (whiskers) of roughness index values (surface area ratio) for surface types mapped on the test site. Total sample size is 12 million raster cells (min. 49,643 per class)

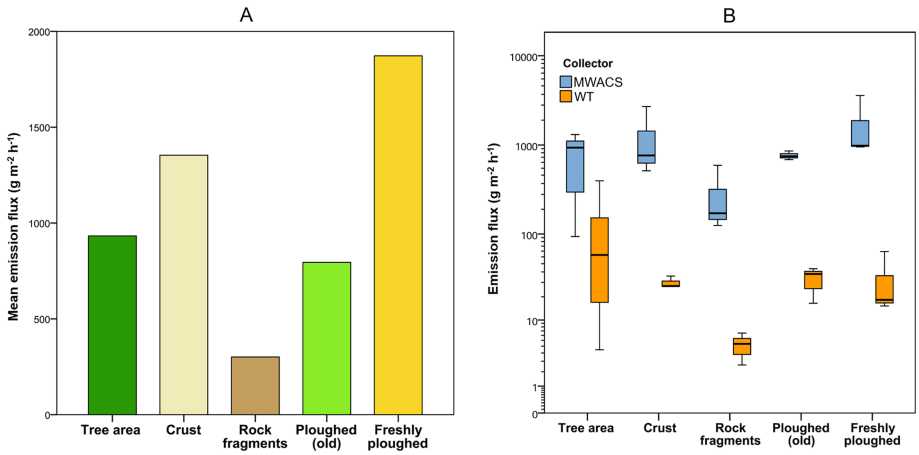

Figure 7. Emission flux derived by wind erosion tests on the test plots: (A) mean values from added collector systems and (B) Mean values from MWACs and WT (run 1) (logarithmic *y*-axis) [Colour figure can be viewed at wileyonlinelibrary.com]

WT-collected material

The results are displayed as cumulative bars for the first and second run to show the temporal development of the emission flux during the first and second test run of 10 min each. The results showed pronounced differences for the two surface types of tree area and rock fragment cover, and very low values for second runs compared with the first runs for all surface types and tests (Tables II and III).

Tree area and rock fragment cover produced the highest and lowest emissions with 153 and 4.75 $g m^{-2} h^{-1}$, respectively. Crust (27.90 $g m^{-2} h^{-1}$) and ploughed (old) (30.42 $g m^{-2} h^{-1}$) showed similar results, but with different portions in the first and second run. The freshly ploughed surface produced slightly higher emission fluxes of 38.85 $g m^{-2} h^{-1}$, and the second highest values for the second run. The crust emission values showed the lowest SD, which might underline the uniformity of the surface and subsequent uniform results for each test run (Table II). The values for the second run (Table III) resembled the relative distribution of the first run for the tree area (39.90 $g m^{-2} h^{-1}$), rock fragments (1.27 $g m^{-2} h^{-1}$) and freshly ploughed surface types (6.95 $g m^{-2} h^{-1}$) but switched for the crust and ploughed (old) types (5.97 and 3.83 $g m^{-2} h^{-1}$, respectively). All surfaces showed strongly reduced emission fluxes after the first 10 min of the test run, and displayed much lower values in the second run (Figure 10A), indicating the typical temporal development of sediment-supply-limited wind erosion events of short duration.

Relation of amount of collected erodible material to substrate and surface characteristics

To investigate RH3, the emission fluxes from all the surface types were tested for potential relations with the quantified plot-specific substrate and surface parameters.

A Shapiro–Wilk test found two sets of the total data to be not normally distributed. Spearman rank coefficient analysis was performed to test for relationships between the collected material and the soil and surface parameters (Table IV).

The fine soil content of the soil substrates appears as a significant parameter in the combined analysis of both collector types (0.736) as well as each type individually (MWACs, 0.752; WT, 0.603). Accordingly, the coarse soil content showed the same significance, but negative correlations. The emission flux correlated positively with the available loose sediment on the surface (grains <2 mm) as well as negatively with the shear strength for both collector types together (0.601 and –0.578, respectively) and for MWACs (0.612 and –0.589, respectively). Vegetation cover correlated negatively with WT emission flux (–0.549).

Discussion

Our experimental study comprised mapping and wind erosion tests on a representative and traditionally managed argan

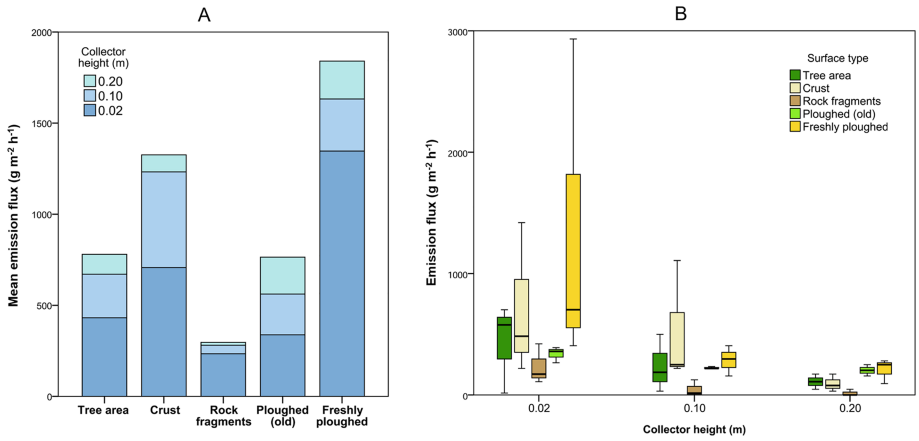

Figure 8. Emission fluxes from MWAC sampler measurements: (A) mean values for different surface types and (B) emission fluxes sorted by collector height and surface type [Colour figure can be viewed at wileyonlinelibrary.com]

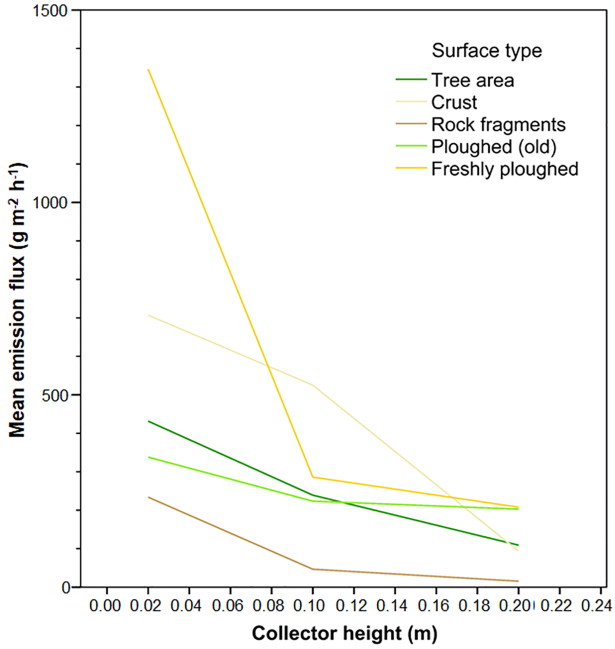

Figure 9. Vertical distribution of transported material collected by MWAC sampler [Colour figure can be viewed at wileyonlinelibrary.com]

woodland site in the Souss Basin to address the following research question: How do specific surface characteristics related to the regional environment influence the susceptibility of open argan woodlands to wind erosion and dust emission?

RH1: The argan woodland environment is composed of different surface types with corresponding specific surface characteristics.

The results finding spatial units of a 1 ha argan woodland surface differing in various aspects support this hypothesis. We defined five surface types based on on-site observation, particularly regarding surface aspects such as crust, coverage and shear resistance. The types varied considerably concerning crust, rock fragment cover and litter cover, but resembled each other in their very low soil water content and percentage vegetation cover. SOC was found to be low for all types except underneath trees, which may also reflect ongoing soil depletion by erosion, as suggested by Sharratt *et al.* (2018). The digital mapping of roughness developed from 1.5 cm-resolution orthophotos supported the definition of these units by differences in roughness indices. The mapping revealed that argan woodlands encompass various surfaces differing on a very small spatial scale and may subsequently determine wind erodibility. Assessment of the spatial distribution of specific surface types is thus necessary to study the regional erosion output potential, particularly for low to medium erosive winds. To achieve this, a larger area of argan woodlands would need to be spatially analysed. The current test location is representative of open argan woodlands on alluvial fans from the High Atlas in the Souss Basin in terms of its physical properties (e.g. grain size distribution, surface cover, substrate depth, tree density and degradation level) with the tested surface types, reflecting different management on a small spatial scale. Between larger regions, surface types or their relative distribution may vary.

RH2: The potential wind erosion of and dust emission from the argan woodland environment are not uniform across the entire area but differ according to surface type.

This research hypothesis is supported by the result that the surface types produced different amounts of emission flux. The comparison of the relative quantities of emission flux revealed that the surfaces most prone to wind erosion were freshly ploughed surfaces and the strongly crusted surfaces with increased runoff activity. The surface least prone to wind erosion was rock fragment cover. These results appeared consistent in terms of case-dependent variability and plausible concerning specific substrate response. The standard deviation (Table II) may be considered acceptable for experimental tests, although the number of experiments and cases per type (three) are not high enough to elaborate statistics.

The freshly ploughed surfaces produced the highest emission flux, which is in line with findings from several other experimental studies (e.g. Ries *et al.*, 2000; Sharratt *et al.*, 2012; Marzen *et al.*, 2019). Ploughing leads to a partial breakdown of crust and clods, generating a comparably high proportion of non-cohesive substrate of the fine sand and silt fractions which are most easily erodible by wind. Depletion of organic matter and the mechanical reduction of aggregate sizes <0.84 mm by ploughing decrease the aggregate stability and further increase the amount of wind-erodible sediment on the surface (Douglas and Goss, 1982; Ries *et al.*, 2000; Tatarko, 2001). Such destruction of the crusted surface is a necessary practice to introduce seeds into the ground and retain rainwater on the field rather than allowing the runoff caused by the minimal infiltration capacity of the crust. Nevertheless, once the crust has been destroyed, wind may act as a powerful erosion agent, particularly under dry soil conditions. This situation is aggravated by an increase and prolongation of drought periods, resulting in an extension of the vulnerable period for

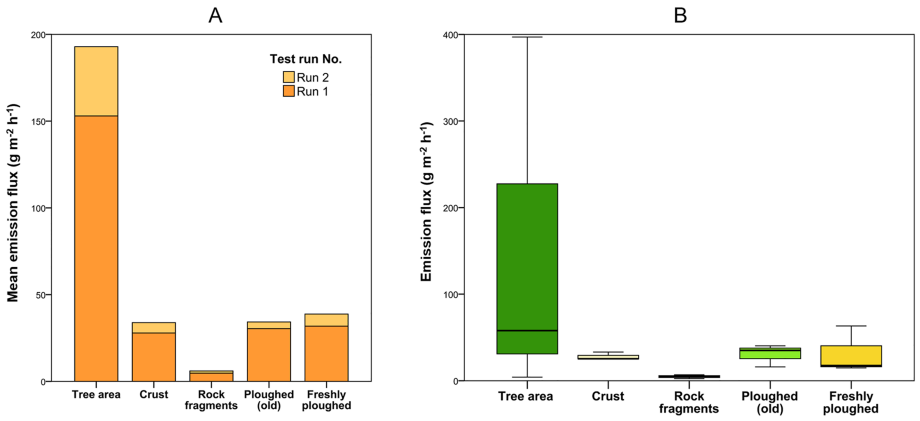

Figure 10. Emission fluxes from WT measurements: (A) mean values for different surface types and runs and (B) emission fluxes sorted by surface types and presented as boxplots [Colour figure can be viewed at wileyonlinelibrary.com]

Table II. Mean emission flux results for collector types and surface types (SD, standard deviation)

Collector/	Mean emission flux ($g m^{-2} h^{-1}$)				
	MWACS		WT		
Surface type (sample size)	Value	SD	Value	SD	Added mean (Figure 7A)
Tree area (3)	779.93	623.16	153.00	213.02	932.93
Crust (3)	1325.88	1195.30	27.90	4.55	1353.78
Rock fragments (3)	296.37	257.73	4.75	2.21	301.12
Ploughed (old) (3)	764.33	86.84	30.42	12.81	794.75
Freshly ploughed (3)	1840.63	1513.06	31.85	27.23	1872.48

tilled fields. Since wind erosion leads to the sorting of soil material and a gradual removal of the finest grain sizes, mainly silt and clay, as well as soil organic matter including a high proportion of soil nutrients (e.g. Gillette, 1977; Bielders *et al.*, 2002; Katra *et al.*, 2016), it is a severe threat to the already depleted soils and substrates of the Souss Region. The effect of tillage during a wind event may act as a trigger for wind erosion, even on surfaces where no wind erosion is measured by experimental procedures, and may be key to the soil loss budget for certain regions. Since one-third of the total area of our representative test site was tilled, the sediment output from similar agriculturally managed argan woodlands is potentially very high. These results support findings from other researchers who found rainfed cultivated fields to be particularly abundant sediment sources in North Africa (Houyou *et al.*, 2014) and Sub-Saharan Africa (e.g. Visser *et al.*, 2004; Touré *et al.*, 2011). Labiadh *et al.* (2013) also point out the significance of the tillage device, finding that modern options trigger stronger erosion than traditional ones. Once precipitation consolidates the top layer of the ploughed area, it becomes much less prone to wind erosion, particularly by airborne transport. This effect may possibly be achieved by some strong fog events that are regularly observed in the region. The ploughed (old) surface featured a 0.5–1 cm thick, rather loosely aggregated physical crust and furrows, protecting the substrate material from erosion. Occasional fresh hoof impressions on the ploughed (old) area reflect the traditional agrosilvopastoral use of the trees as a biomass resource for browsing goats and sheep, particularly during periods of drought (Le Polain de Waroux and Lambin, 2012). The hooves produce easily available soil material by destroying the crust, which is however trapped in depressions. Lybbert *et al.* (2011) found that grazing herds were controlled during the fruit harvesting season, after which browsing became uncontrolled. They found that argan trees were well adapted to arid conditions, surviving in a dormant state for several years during extreme drought but being quite vulnerable during lesser drought conditions that do not trigger this dormant state.

The crust area was found to be the second highest emission source, despite the fact that both physical and biological crusts generally reduce wind erosion to a minimum (e.g. McKenna-Neuman *et al.*, 1996; Singer and Shainberg, 2004; Zobeck, 1991). Higher emission rates were found only if the crust was destroyed e.g. by cars (Gillette *et al.*, 1982) or trampling by military personnel (Belnap *et al.*, 2007) or animals (Marzen *et al.*, 2019). Trampling by animals is a very likely origin of the eroded material at our test site, thus producing the second highest sediment yield. Apart from material deflated from nearby freshly ploughed areas, material may also originate from regional and supra-regional sediment sources. Puy *et al.* (2018) detected manifold sources for recently deposited particles, including adjacent areas as well as a considerable percentage of remote dust sources possibly connected to peri-Saharan regions and the Sahara.

Less important sources of the easily available material may be prior water erosion events including inter-rill erosion and, to a minor extent, on-site weathering. At our test site, which represents a traditionally managed argan woodland, this surface type covers ca. 14% of the total area. It is important to note the possible distribution function for supra-regionally dust emissions from this surface type instead of providing a sediment sink.

The tree area surface type produced a high emission flux with a high proportion of loose organic material. During summer and autumn, it may even act as a protection for underlying mineral sediments. Kirchhoff *et al.* (2019a) found that tree-covered areas in argan woodlands show higher values of soil organic matter and lower erodibility compared with inter-tree areas. Our results support this general distinction insofar as soil surface properties and emission fluxes vary only slightly compared with all other surface types. The high percentage of organic litter is available for mineralization by soil organisms, leading to the highest measured SOC and aggregate stability of all the tested samples. Since SOC has been found to decrease wind erosion potential (Sirjani *et al.*, 2019), the high content underneath the trees may explain the comparably low amount of measured wind-erodible material despite the fact that this substrate has much lower shear resistance than other surface types.

Based on the identification of different surface types, we applied an experimental test setup and relatively quantified the potential wind erosion associated with each surface type.

Table III. Mean emission fluxes for collector types, heights, run 1 + 2 and surface types

Collector	Mean horizontal flux ($g m^{-2} h^{-1}$)						
	Modified Wilson and Cook samplers				Wedge traps		
Surface type (sample size)	0.02 m	0.10 m	0.20 m	Total	Run 1	Run 2	Total
Tree area (3)	431.56	239.18	109.19	779.93	153.00	39.90	192.90
Crust (3)	707.14	525.15	93.59	1325.88	27.90	5.97	33.87
Rock fragments (3)	233.98	46.80	15.60	296.37	4.75	1.27	6.02
Ploughed (old) (3)	337.97	223.58	202.78	764.33	30.42	3.83	34.25
Freshly ploughed (3)	1346.68	285.97	207.98	1840.63	31.85	6.95	38.80

Table IV. Correlations (Spearman's rho) between emission fluxes and soil and surface parameters significant at *0.05 and **0.01 level (two-tailed)

	Surface parameters							Substrate parameters				
	Litter	Veg.	Crust	Grain <2 mm	Rock fragments	Roughness	Shear strength	fine soil (< 2 mm)	coarse soil (>2 mm)	Soil moisture	Percolation stability	SOC
Spearman's rho	(%)	(%)	(%)	(%)	(%)	(C_r index)	(kg cm^{-2})	(%)	(%)	(%)	(ml/10 min)	(%)
Emission flux (total)												
Correlation coefficient	–0.397	–0.417	–0.045	0.601*	–0.056	0.293	–0.578*	0.736**	–0.736**	0.020	–0.241	–0.241
Sig. (two-tailed)	0.143	0.122	0.873	0.018	0.843	0.289	0.023	0.001	0.001	0.943	0.388	0.388
N	15	15	15	15	15	15	15	15	15	15	15	15
Emission flux (MWACS)												
Correlation coefficient	–0.411	–0.417	–0.065	0.612*	–0.042	0.329	–0.589*	0.752**	–0.752**	–0.004	–0.269	–0.269
Sig. (two-tailed)	0.128	0.122	0.818	0.015	0.883	0.232	0.020	0.001	0.001	0.990	0.333	0.333
N	15	15	15	15	15	15	15	15	15	15	15	15
Emission flux (WT)												
Correlation coefficient	0.026	–0.549*	0.336	0.499	–0.388	0.107	–0.426	0.603*	–0.603*	–0.072	–0.151	–0.151
Sig. (two-tailed)	0.927	0.034	0.221	0.058	0.153	0.704	0.113	0.017	0.017	0.799	0.591	0.591
N	15	15	15	15	15	15	15	15	15	15	15	15

RH3: Material collected from wind erosion tests is significantly related to substrate and surface characteristics.

The results only approximately support this research hypothesis, since the correlation analysis revealed only minor information about the relations between the erodible material collected from all the surface types and their substrate and surface parameters. This was caused by the relatively small number of samples (15) and partly by the very small ranges of the measured values. The correlation analysis revealed that a high fine soil content of the substrate was a major factor for high emission flux. Erodible material was also positively correlated with the fine material available on the surface, as well as negatively with shear strength. Vegetation cover showed a slight negative correlation with emission flux as measured using wedge traps. These results may be interpreted such that the potential for wind erosion depends mainly on the available transportable fine soil material, a related low shear resistance of the surface and sparse vegetation cover.

Answering this research question, we found that the potential erosion dynamics quantified on the representative units reflected recent land use and land-use change.

Remote-sensing studies have revealed continuous degradation of the argan woodlands over recent decades, with increasing fragmentation of important stabilizing vegetation such as *Genista pseudopilosa* and *Artemisia herba-alba* (Kouba *et al.*, 2018) and a drastic decrease in the population density of *Argania spinosa* (Le Polain de Waroux and Lambin, 2012). Most studies have found desertification clearly associated with high population and livestock pressure (del Barrio *et al.*, 2016; Lahlaoi *et al.*, 2017), including intensifying water scarcity due to declining aquifer recharge (Jilali, 2014) and the subsequent risk of water shortages (Johannsen *et al.*, 2016), which is further aggravated by climate change (Van Dijck *et al.*, 2006). Although Chakhchar *et al.* (2015) found the genetic variety of inland argan ecotypes to be more drought tolerant compared with varieties from coastal areas, different approaches for rejuvenation of argan sites in the Souss Basin have not been successful for several reasons, the most important being a lack of sufficient protection against browsing herds and insufficient maintenance of young plants. In the medium term, older argan trees will thus disappear, increasing the area between individuals. In combination with the projected decrease and variability of precipitation, which has already been found to increase water erosion (Simonneaux *et al.*, 2015), the bare surface will extend to large areas.

Besides all its other ecological and socio-economic effects, this decrease in surface cover is likely to enhance wind erosion and dust emission dramatically. The trees and bushes will cease to provide direct protection as wind cover with reduced wind speeds creating deposition areas among and on the lee side of patchily distributed plants. A loss of trees leads to an extension of the wind fetch distance, which will probably have the greatest impact on particle mobilization due to increased saltation and thus abrasion by sand particles. Due to its high impact energy, this sandblast effect may even outweigh a possibly increased development of physical or biological crust, particularly since our results show that the crusted areas are among the most productive surfaces. An indirect effect would be further degradation of soils and substrates due to a lack of organic input in terms of organic substances and activity. This could lead to reduced aggregate development and stability, in turn increasing the erodibility by wind and water. Our results suggest that redistribution of organic material from the argan trees beyond the area of its production might be an important fertilizing process for the surrounding areas. This means that a continued loss of argan trees would also negatively affect substrate conditions over a larger area, presumably in the main wind directions covering the Souss Basin from the south west to north east.

However, we generally state that such point values on small spatial and temporal scales derived from this and other experimental devices are not adequate to perform extrapolations to greater temporal and spatial scales. This is due to the physical limitations of the experimental setting, including the abstracted physical parameters concerning the erosive agent as well as the small number of tested surfaces compared with the regional extent of the investigation area. In particular, the data are also not adequate for use in landscape or landform development assessments.

Conclusion

Mapping of an endemic argan woodland site in the Souss Basin, south Morocco revealed various surface types interwoven on a very small spatial scale. These surface types were found to produce differing emission fluxes during experimental wind erosion measurements:

1 Freshly ploughed surfaces under agrosilvopastoral management produced the highest erosion values. The dry loamy substrate with low shear resistance was highly susceptible to wind erosion at a comparably low velocity and could dramatically increase the total regional sediment yield.
2 Strongly crusted surfaces produced the second highest sediment yield, demonstrating the high erosive potential of surfaces that are very typical for the whole region. While strongly crusted and highly shear resistant, these surfaces may act as a sediment distributor for temporarily stored supra-regionally transported dust. If trees and associated structures further cease to function as wind-breaking obstacles and sediment catchers, these surfaces may become considerable sediment sources in the medium term.
3 Tree-shaded areas were found to produce emission fluxes with a low proportion of mineral content and a high proportion of organic material. The litter cover may protect the underlying substrate from erosion and enhance the substrate structure by increasing the aggregate stability and enhancing soil biological activity. The litter, particularly when crushed, may act as a fertilizer even over supra-regional accumulation areas.
4 Old ploughed surfaces that have already re-established a slight surface crust due to precipitation or strong fog events were found to exhibit a comparatively low erodibility. The traditional agricultural management is thus in line with soil conservation, since traditional ploughing happens in the prospect of imminent rain. Climate-change-related increased variability and generally decreasing rain leads to the potential threat of wind erosion and dust emission.
5 The surface least prone to wind erosion was that covered with rock fragments. On a larger scale, these areas may even act as sediment catchers which are valuable for the entire woodland.

The high erosion values found on freshly ploughed surfaces confirm agricultural management as a paramount trigger inducing severe consequences for environmental, economic and societal issues. Adapted land management would therefore have great potential as a valuable tool to mitigate the possible impacts of land-use change, as well as climate-change-related shifts in wind and rainfall patterns. Based on our results, conservation of argan trees and the specific woodland character is an urgent concern to prevent severe dust production and dust

distribution and to maintain the sediment source potential of this vulnerable environment at the fringes of the Sahara Desert.

Acknowledgements—We would like to thank the Deutsche Forschungsgemeinschaft (DFG), grant numbers RI 835/24-1 and MA 2549/6-1, for funding this research.

We also acknowledge the support of the laboratories of Trier University as well as of the Université Ibn Zohr Agadir, weatheronline.co.uk for providing the wind data and would like to thank Lars Engelmann and Abdellatif Hanna for their considerable help during data acquisition in the field. Open access funding enabled and organized by Projekt DEAL.

Data Availability Statement

The datasets used and/or analysed during the current study are available from the corresponding author on reasonable request.

Conflict of Interest

The authors declare that there are no conflicts of interest.

References

AGR/DAF (2002) The National Action Plan for Combating Desertification Report. Ministry of Agriculture, Rural Development, Water and Forestry. Rabat.

Aït Hssaine A. 2000. Evolution géomorphologique du piémont sud-atlasique dans la région de Taroudant (SW-Maroc) au cours du Tertiaire et du Pléistocène inférieur. *Bulletin de l'Institut Scientifique* **22**: 17–28.

Aït Hssaine A, Bridgland D. 2009. Pliocene-Quaternary fluvial and aeolian records in the Souss basin, southwest Morocco: A geomorphological model. *Global and Planetary Change* **68**(4): 288–296. https://doi.org/10.1016/j.gloplacha.2009.03.002

Ait Kadi M, Ziyad A. 2018. Integrated Water Resources Management in Morocco. In *Global Water Security*, World Water Council (ed). Springer: Singapore; 143–163.

Auerswald K. 1995. Percolation Stability of Aggregates from Arable Topsoils. *Soil Science* **159**: 142–148.

Bagnold RA. 1941. *The physics of blown sand and desert dunes*. Methuen: London.

Belnap J, Phillips SL, Herrick JE, Johansen JR. 2007. Wind erodibility of soils at Fort Irwin, California (Mojave Desert), USA, before and after trampling disturbance: implications for land management. *Earth Surface Processes and Landforms* **32**: 75–84. https://doi.org/10.1002/esp.1372

Bielders CL, Rajot J-L, Amadou M. 2002. Transport of soil and nutrients by wind in bush fallow land and traditionally managed cultivated fields in the Sahel. *Geoderma* **109**: 19–39.

Bouabid R, Rouchdi M, Badraoui M, Diab A, Louafi S. 2010. Assessment of Land Desertification Based on the MEDALUS Approach and Elaboration of an Action Plan: The Case Study of the Souss River Basin, Morocco. In *Land Degradation and Desertification: Assessment, Mitigation and Remediation*, Zdruli P, Pagliai M, Kapur S, Faz Cano A (eds). Springer: Heidelberg, Germany; 131–145.

Bullard J, Baddock M. 2019. Dust. Sources, Entrainment, Transport. In *Aeolian Geomorphology: A New Introduction*, Livingstone I, Warren A (eds). Wiley-Blackwell: Oxford, UK; 81–106.

Chakhchar A, Wahbi S, Lamaoui M, Ferradous A, El Mousadik A, Ibnsouda-Koraichi S et al. 2015. Physiological and biochemical traits of drought tolerance in Argania spinosa. *Journal of Plant Interactions* **10**(1): 252–261. https://doi.org/10.1080/17429145.2015.1068386

Chakir L, Aït Hssaine A, Bridgland D. 2014. Morphogenesis and morphometry of alluvial fans in the High Atlas, Morocco: A geomorphological model of the fans of the Wadi Beni Mhammed, Souss valley. *International Journal of Environment* **3**(3): 294–311. https://doi.org/10.3126/ije.v3i3.11090

Chepil WS. 1945. Dynamics of wind erosion: I. Nature of movement of soil by wind. *Soil Science* **60**(4): 305–320.

Chepil WS. 1960. Conversion of Relative Field Erodibility to Annual Soil Loss by Wind. *Soil Science Society of America Journal* **24**(2): 143–145. https://doi.org/10.2136/sssaj1960.03615995002400020022x

Chepil WS, Woodruff NP. 1963. The Physics of Wind Erosion and its Control. *Advances in Agronomy* **15**: 211–302. https://doi.org/10.1016/S0065-2113(08)60400-9

del Barrio G, Sanjuan M, Hirche A, Yassin M, Ruiz A, Ouessar M, Puigdefabregas J. 2016. Land degradation states and trends in the northwestern Maghreb drylands, 1998–2008. *Remote Sensing* **8**(7): 603. https://doi.org/10.3390/rs8070603

Darboux F, Davy P, Gascuel-Odoux C, Huang C. 2002. Evolution of soil surface roughness and flowpath connectivity in overland flow experiments. *Catena* **46**(2–3): 125–139. https://doi.org/10.1016/S0341-8162(01)00162-X

De Oro LA, Colazo JC, Avecilla F, Buschiazzo DE, Asensio C. 2019. Relative soil water content as a factor for wind erodibility in soils with different texture and aggregation. *Aeolian Research* **37**: 25–31. https://doi.org/10.1016/j.aeolia.2019.02.001

Dong Z, Liu X, Wang H, Zhao A, Wang X. 2003. The flux profile of a blowing sand cloud: a wind tunnel investigation. *Geomorphology* **49**: 219–230. https://doi.org/10.1016/S0169-555X(02)00170-8

Douglas JT, Goss MJ. 1982. Stability and organic matter content of surface soil aggregates under different methods of cultivation and in grassland. *Soil and Tillage Research* **2**(2): 155–175. https://doi.org/10.1016/0167-1987(82)90023-X

Duniway MC, Pfennigwerth A, Fick S, Nauman T, Belnap J, Barger N. 2019. Wind erosion and dust from US drylands: a review of causes, consequences, and solutions in a changing world. *Ecosphere* **10**(3): e02650. https://doi.org/10.1002/ecs2.2650

FAO AQUASTAT (2015). *Country Profile - Morocco*. Retrieved from: http://www.fao.org/aquastat/en/countries-and-basins/country-profiles/country/MAR

Fister W, Iserloh T, Ries JB, Schmidt RG. 2012. A portable wind and rainfall simulator for in situ soil erosion measurements. *Catena* **91**: 72–84. https://doi.org/10.1016/j.catena.2011.03.002

Funk R. 2016. Assessment and Measurement of Wind Erosion. In *Novel Methods for Monitoring and Managing Land and Water Resources in Siberia*, Mueller L, Sheudshen AK, Eulenstein F (eds). Springer International Publishing: Basel, Switzerland.

Gillette DA. 1977. Fine particulate emissions due to wind erosion. *Transactions of the ASAE* **20**(5): 890–897. https://doi.org/10.13031/2013.35670

Gillette DA, Adams J, Muhs DR, Kihl R. 1982. Threshold friction velocities and rupture moduli for crusted desert soils for the input of soil particles into the air. *Journal of Geophysical Research Atmospheres* **87**(C11): 9003–9016. https://doi.org/10.1029/JC087iC11p09003

Goossens D, Offer Z, London G. 2000. Wind tunnel and field calibration of five Aeolian sand traps. *Geomorphology* **35**: 233–252. https://doi.org/10.1016/S0169-555X(00)00041-6

Goossens D, Nolet C, Etyemezian V, Duarte-Campos L, Bakker G, Riksen M. 2018. Field testing, comparison, and discussion of five aeolian sand transport measuring devices operating on different measuring principles. *Aeolian Research* **32**: 1–13. https://doi.org/10.1016/j.aeolia.2018.01.001

Goudie AS. 2014. Desert dust and human health disorders. *Environment International* **63**: 101–113. https://doi.org/10.1016/j.envint.2013.10.011

Hoffmann C, Funk R, Reiche M, Li Y. 2011. Assessment of extreme wind erosion and its impacts in Inner Mongolia, China. *Aeolian Research* **3**: 343–351. https://doi.org/10.1016/j.aeolia.2011.07.007

Houyou Z, Bielders CL, Benhorma HA, Dellal A, Boutemdje A. 2014. Evidence of strong land degradation by wind erosion as a result of rainfed cropping in the Algerian steppe: a case study at Laghouat. *Land degradation and Development* **27**(8): 1788–1796. https://doi.org/10.1002/ldr.2295

Houzir, M., Mokass, M., & Schalatek, L. (2016). Climate Governance and the Role of Climate Finance in Morocco. Retrieved from Heinrich Böll Stiftung website: https://us.boell.org/sites/default/files/morocco_study_climate_governance_final_english_nov.2.pdf

Hssaisoune, M., Boutaleb, S., Benssaou, M., Bouaakkaz, B., & Bouchaou, L. (2016). Physical Geography, Geology, and Water Resource Availability of the Souss-Massa River Basin. In: R. Choukr-Allah, R. Ragab, L. Bouchaou, & D. Barceló (Eds.), *The*

Souss-Massa River Basin, Morocco (pp. 27-56). Basel, Switzerland: Springer International Publishing. https://doi.org/10.1007/698_2016_68

Hssaisoune M, Bouchaou L, Sifeddine A, Bouimetarhan I, Chehbouni A. 2020. Moroccan groundwater resources and evolution with global climate changes. *Geosciences* **10**(2): 81.

IBM Corp. *Released 2017. IBM SPSS Statistics for Windows, (Version 25.0) [Computer Software]*. IBM Corp: Armonk, NY.

IPCC. 2019, In press. Summary for Policymakers. In *Climate Change and Land: an IPCC special report on climate change, desertification, land degradation, sustainable land management, food security, and greenhouse gas fluxes in terrestrial ecosystems*, Shukla PR, Skea J, Buendia EC, Masson-Delmotte V, Pörtner H-O, Roberts DC et al. (eds).

Iserloh T, Fister W, Marzen M, Seeger M, Kuhn NJ, Ries JB. 2013. The role of wind-driven rain for soil erosion – an experimental approach. *Zeitschrift Für Geomorphologie Supplementary Issues* **57**: 193–201. https://doi.org/10.1127/0372-8854/2012/S-00118

Jenness, J. (2013) DEM Surface Tools [Computer software]. Jenness Enterprises. Available at: http://www.jennessent.com/arcgis/surface_area.htm

Jilali A. 2014. Impact of climate change on the Figuig aquifer using a numerical model: Oasis of 1 Eastern Morocco. *Journal of Biology and Earth Sciences* **4**(1): 16–24.

Johannsen I, Hengst J, Goll A, Höllermann B, Diekkrüger B, Johannsen IM, Diekkrüger B. 2016. Future of water supply and demand in the middle Drâa Valley, Morocco, under climate and land use change. *Water* **8**(8): 313. https://doi.org/10.3390/w8080313

Jones A, Breuning-Madsen H, Brossard M, Dampha A, Deckers J, Dewitte O et al. (eds). 2013. *Soil Atlas of Africa*. European Commission, Publications Office of the European Union: Luxembourg.

Katra I, Gross A, Swet N, Tanner S, Krasnov H, Angert A. 2016. Substantial dust loss of bioavailable phosphorus from agricultural soils. *Scientific Reports* **6**: 24736. https://doi.org/10.1038/srep24736

Kirchhoff M, Engelmann L, Zimmermann LL, Seeger M, Marzolff I, Aït Hssaine A, Ries JB. 2019a. Geomorphodynamics in argan woodlands, south Morocco. *Water* **11**: 2193. https://doi.org/10.3390/w11102193

Kirchhoff M, Peter KD, Aït Hssaine A, Ries JB. 2019b. Land use in the Souss region, South Morocco and its influence on wadi dynamics. *Zeitschrift für Geomorphologie* **62**: 137–160. https://doi.org/10.1127/zfg_suppl/2019/0525

Kok JF, Parteli EJR, Michaels TI, Bou Karam D. 2012. The physics of wind-blown sand and dust. *Reports on Progress in Physics* **75**(10): 106901. https://doi.org/10.1088/0034-4885/75/10/106901

Köhn M. 1929. Korngrößenanalyse mittels Pipettenanalyse. *Tonindustrie-Zeitung* **53**: 729–731.

Kouba Y, Gartzia M, El Aich A, Alados CL. 2018. Deserts do not advance, they are created: Land degradation and desertification in semiarid environments in the Middle Atlas, Morocco. *Journal of Arid Environments* **158**: 1–8. https://doi.org/10.1016/j.jaridenv.2018.07.002

Kuhn A, Heidecke C, Roth A, Goldbach H, Burkhardt J, Linstädter A et al. 2010. Importance of resource management for livelihood security under Climate Change in Southern Morocco. In *Impacts of Global Change on the Hydrological Cycle in West and Northwest Africa*, Speth P, Christoph M, Diekkrüger B (eds). Springer: Heidelberg, Germany; 566–591.

Labiadh M, Bergametti G, Kardous M, Perrier S, Grand N, Attoui B et al. 2013. Soil erosion by wind over tilled surfaces in South Tunisia. *Geoderma* **202-203**: 8–17. https://doi.org/10.1016/j.geoderma.2013.03.007

Lahlaoi H, Rhinane H, Hilali A, Lahssini S, Moukrim S. 2017. Desertification Assessment Using MEDALUS Model in Watershed Oued El Maleh, Morocco. *Geosciences* **7**(3): 50. https://doi.org/10.3390/geosciences7030050

Lefhaili, A. (2015). Evaluation des ressources forestières mondiales 2015. Rapport national, Maroc. FAO: 11.

Le Polain de Waroux Y, Lambin EF. 2012. Monitoring degradation in arid and semi-arid forests and woodlands: The case of the argan woodlands (Morocco). *Applied Geography* **32**: 777–786. https://doi.org/10.1016/j.apgeog.2011.08.005

Leys J, McTainsh GH. 1996. Sediment fluxes and particle grain-size characteristics of wind-eroded sediments in Southeastern Australia. *Earth Surface Processes and Landforms* **21**(7): 661–671. https://doi.org/10.1002/(SICI)1096-9837(199607)21:7<661::AID-ESP663>3.0.CO;2-4

Lybbert TJ, Magnan N, Aboudrare A. 2010. Household and local forest impacts of Morocco's argan oil bonanza. *Environment and Development Economics* **15**(4): 439–464. https://doi.org/10.1017/S1355770X10000136

Lybbert TJ, Aboudrare A, Chaloud D, Magnan N, Nash M. 2011. Booming markets for Moroccan argan oil appear to benefit some rural households while threatening the endemic argan forest. *PNAS* **108**(34): 13963–13968. https://doi.org/10.1073/pnas.1106382108

Marzen M, Iserloh T, de Lima JLMP, Fister W, Ries JB. 2017. Impact of severe rain storms on soil erosion: Experimental evaluation of wind-driven rain and its implications for natural hazard management. *Science of the Total Environment* **15**: 502–513. https://doi.org/10.1016/j.scitotenv.2017.02.190

Marzen M, Iserloh T, Fister W, Seeger M, Rodrigo Comino J, Ries JB. 2019. On-site water and wind erosion experiments reveal relative impact on total soil erosion. *Geosciences* **9**(11): 478. https://doi.org/10.3390/geosciences9110478

Mbagwu JSC, Auerswald K. 1999. Relationship of percolation stability of soil aggregates to land use, selected properties, structural indices and simulated rainfall erosion. *Soil and Tillage Research* **50**(3-4): 197–206. https://doi.org/10.1016/S0167-1987(99)00006-9

McGregor HV, Dupont LM, Stuut JBW, Kuhlmann H. 2009. Vegetation change, goats, and religion: a 2000-year history of land use in southern Morocco. *Quaternary Science Reviews* **28**(15-16): 1434–1448. https://doi.org/10.1016/j.quascirev.2009.02.012

McKenna-Neumann C, Maxwell C, Bolton JW. 1996. Wind transport of sand surface with photoautotrophic microorganisms. *Catena* **27**: 229–247.

Middleton NJ. 2017. Desert dust hazards: A global review. *Aeolian Research* **24**: 53–63. https://doi.org/10.1016/j.aeolia.2016.12.001

Mendez MJ, Funk R, Buschiazzo DE. 2016. Efficiency of Big Spring Number Eight (BSNE) and Modified Wilson and Cook (MWAC) samplers to collect PM10, PM2.5 and PM1. *Aeolian Research* **21**: 37–44. https://doi.org/10.1016/j.aeolia.2016.02.003

Montanarella L, Pennock DJ, McKenzie N, Badraoui M, Chude V, Baptista I, Vargas R. 2016. World's soils are under threat. *SOIL* **2**: 79–82. https://doi.org/10.5194/soil-2-79-2016

Peter KD, d'Oleire-Oltmanns S, Ries JB, Marzolff I, Aït Hssaine A. 2014. Soil erosion in gully catchments affected by land-levelling measures in the Souss basin, Morocco, analysed by rainfall simulation and UAV remote sensing data. *Catena* **113**: 24–40. https://doi.org/10.1016/j.catena.2013.09.004

Puy A, Herzog M, Escriche P, Marouche A, Oubana Y, Bubenzer O. 2018. Detection of sand encroachment patterns in desert oases. The case of Erg Chebbi (Morocco). *Science of The Total Environment* **642**: 241–249. https://doi.org/10.1016/j.scitotenv.2018.05.343

Ravi S, D'Odorico P, Over TM, Zobeck TM. 2004. On the effect of air humidity on soil susceptibility to wind erosion: The case of air-dry soils. *Geophysical Research Letters* **31**(9). https://doi.org/10.1029/2004GL019485

Ries JB, Langer M, Rehberg C. 2000. Experimental investigations on water and wind erosion on abandoned fields and arable land in the central Ebro Basin, Aragón/Spain. *Zeitschrift für Geomorphologie Supplementary Issues* **121**: 91–108.

Saleh A. 1993. Soil roughness measurement: Chain method. *Journal of Soil and Water Conservation* **48**(6): 527–529.

Sharratt B, Wendling L, Feng G. 2012. Surface characteristics of a wind-blown soil altered by tillage intensity during summer fallow. *Aeolian Research* **5**: 1–7. https://doi.org/10.1016/j.aeolia.2012.02.002

Sharratt BS, Kennedy AC, Hansen JC, Schillinger WF. 2018. Soil carbon loss by wind erosion of summer fallow fields in Washington's dryland wheat region. *Soil & Water Management & Conservation* **82**(6): 1551–1558. https://doi.org/10.2136/sssaj2018.06.0214

Simonneaux V, Cheggour A, Deschamps C, Mouillot F, Cerdan O, Le Bissonnais Y. 2015. Land use and climate change effects on soil erosion in a semi-arid mountainous watershed (High Atlas, Morocco). *Journal of Arid Environments* **122**: 64–75. https://doi.org/10.1016/j.jaridenv.2015.06.002

Singer MJ, Shainberg I. 2004. Mineral soil surface crusts and wind and water erosion. *Earth Surface Processes and Landforms* **29**(9): 1065–1075. https://doi.org/10.1002/esp.1102

Sirjani E, Sameni A, Moosavi AA, Mahmoodabadi M, Laurent B. 2019. Portable wind tunnel experiments to study soil erosion by wind and its link to soil properties in the Fars province, Iran. *Geoderma* **333**: 69–80. https://doi.org/10.1016/j.geoderma.2018.07.012

Stephan R, Marzolff I, Kirchhoff M. 2019. UAV-based remote sensing in argan woodlands, Morocco. *Geophysical Research Abstracts* **21**: 6615.

Tatarko J. 2001. Soil aggregation and wind erosion: processes and measurements. *Annals of Arid Zone* **40**(3): 251–263.

Touré AA, Rajot J-L, Garba Z, Marticorena B, Petit C, Sebag D. 2011. Impact of very low crop residues cover on wind erosion in the Sahel. *Catena* **85**(3): 205–214. https://doi.org/10.1016/j.catena.2011.01.002

UNESCO (2002). Biosphere Reserve Information, Morocco, Arganeraie. Retrieved from: http://www.unesco.org/mabdb/br/brdir/directory/biores.asp?code=MOR+01&mode=all

UNESCO (2015). Argan, Practices and Know-How Concerning the Argan Tree. Retrieved from: www.unesco: Culture/ich/en/RL/00955.

Van Dijck SJE, Laouina A, Carvalho AV, Loos S, Schipper AM, Van der Kwast H et al. 2006. Desertification in northern Morocco due to effects of climate change on groundwater recharge. In *Desertification in the Mediterranean Region. A Security Issue*, Kepner WG, Rubio JL, Mouat DA, Pedrazzini F (eds). Springer: Dordrecht, Netherlands; 549–577.

Visser SM, Sterk G, Snepvangers JJJC. 2004. Spatial variation in wind-blown sediment in geomorphic units in northern Burkina Faso using geostatistical mapping. *Geoderma* **120**(1-2): 95–107. https://doi.org/10.1016/j.geoderma.2003.09.003

Weatheronline.co.uk. n.d. Retrieved from: https://www.weatheronline.co.uk/weather/maps/city?LANG=en&PLZ=_____&PLZN=_____&WMO=60253&CONT=afri&R=0&LEVEL=162&REGION=0011&LAND=MC&MOD=tab&ART=WST&NOREGION=1

Wilson SJ, Cooke RU. 1980. Wind erosion. In *Soil Erosion*, Kirkby MJ, Morgan RPC (eds). Wiley: Chichester, UK; 217–251.

Wirtz S, Iserloh T, Marzen M, Fister W. 2020. Chapter 8. Experimental field methods to quantify soil erosion by water and wind-driven-rain. In *Field Measurement Methods in Soil Science*, Wessel-Bothe S, Weihermüller L (eds). Gebr. Borntraeger Science Publishers: Stuttgart, Germany; 165–190.

Zobeck TM. 1991. Soil properties affecting wind erosion. *Journal of Soil and Water Conservation* **46**(2): 112–118.